Hydroxysteroid 17-beta dehydrogenase 13 *(Hsd17b13)* knockdown attenuates liver steatosis in high-fat diet obese mice

Shehroz Mahmood[1,2], Nicola Morrice[1,2,4], Dawn Thompson[1,2], Sara Milanizadeh[1,2], Sophie Wilson[1,2], Philip D. Whitfield[5], George D. Mcilroy[1,3], Justin J. Rochford[1,3], Nimesh Mody[1,2]

1. Aberdeen Cardiovascular & Diabetes Centre,

2. Institute of Medical Sciences,

3. The Rowett Institute,

1,2,3. School of Medicine, Medical Sciences & Nutrition, University of Aberdeen, Aberdeen, AB25 2ZD, Scotland, UK

4. Centre for Genome Enabled Biology & Medicine, University of Aberdeen, Aberdeen, AB24 3UU, Scotland, UK

5. Glasgow Polyomics, University of Glasgow, Garscube Campus, Glasgow, G61 1QH, UK.

Correspondence: Nimesh Mody, n.mody@abdn.ac.uk

RESEARCH ARTICLE

RUNNING HEAD:

Hsd17b13 RNAi knockdown attenuates liver steatosis in mice

ABSTRACT

Hydroxysteroid 17-beta dehydrogenase 13 (*HSD17B13*) loss-of-function gene variants are associated with decreased risk of 'metabolic dysfunction-associated steatotic liver disease' (MASLD). Our RNA-seq analysis of steatotic liver from obese mice -/+ Fenretinide treatment identified major beneficial effects of Fenretinide on hepatic gene expression including *Hsd17b13*. We sought to determine the relationship between Hsd17b13 expression and MASLD and to validate it as a therapeutic target by liver-specific knockdown. *Hsd17b13* expression, which is unique to hepatocytes and associated with the lipid-droplet, was elevated in multiple models of MASLD and normalised with prevention of obesity and steatotic liver. Direct, liver-specific, shRNA-mediated knockdown of *Hsd17b13* (shHsd17b13) in high-fat diet (HFD)-obese mice, markedly improved hepatic steatosis with no effect on body weight, adiposity or glycaemia. shHsd17b13 decreased elevated serum ALT, serum FGF21 levels and markers of liver fibrosis e.g. *Timp2*. shHsd17b13 knockdown in HFD-obese mice and Hsd17b13 overexpression in cells reciprocally regulated expression of lipid metabolism genes e.g. *Cd36*. Global lipidomic analysis of liver tissue revealed a major decrease in diacylglycerols (e.g. DAG 34:3) with shHsd17b13 and an increase in phosphatidylcholines containing polyunsaturated fatty acids (PUFA) e.g. PC 34:3 and PC 42:10. Expression of key genes involved in phospholipid and PUFA metabolism e.g. *Cept1*, were also reciprocally regulated suggesting a potential mechanism of Hsd17b13 biological function and role in MASLD. In conclusion, *Hsd17b13* knockdown in HFD-obese adult mice was able to alleviate MASLD via regulation of fatty acid and phospholipid metabolism, thereby confirming HSD17B13 as a genuine therapeutic target for MASLD and development of liver fibrosis.

NEW & NOTEWORTHY

RNA-seq analysis of steatotic liver identified beneficial effects of Fenretinide on hepatic gene expression including Hsd17b13. Liver-specific shRNA knockdown of Hsd17b13 (shHsd17b13) in obese mice markedly improved hepatic steatosis and markers of liver health e.g. Fgf21. Hsd17b13 influenced expression of lipid/phospholipid metabolism genes e.g. Cd36 and Cept1 and phosphatidylcholines PC 34:3 and PC 42:10. Our study suggests a mechanism of HSD17B13's biological function and that the translational potential of targeting HSD17B13 for MASLD/MASH is strong.

Keywords: Fenretinide, fibrosis, non-alcoholic fatty liver disease (NAFLD), Hydroxysteroid 17-Beta Dehydrogenase 13 (Hsd17b13), phospholipids

---

INTRODUCTION

Metabolic dysfunction-associated steatotic liver disease (MASLD), previously termed non-alcoholic fatty liver disease (NAFLD) is a common complication associated with obesity and diabetes. MASLD can progress to the more severe metabolic dysfunction-associated steatohepatitis (MASH), previously termed non-alcoholic steatohepatitis (NASH) and therefore requires urgent therapeutic attention (1). MASLD is characterised by an accumulation of triglycerides in the liver and is estimated to affect 25-30% of the global population as well as up to 90% of patients classed as morbidly obese (1). Currently, there are no approved therapeutics available for MASLD other than dietary and lifestyle interventions, however human trials suggest medicines with known benefits against obesity and diabetes may be useful to also treat MASLD (2). In addition, several novel pharmacologic therapies are in various phases of clinical development for the specific treatment of MASLD/MASH (3).

Several studies including human genome-wide association and multi-omics data analysis have identified genes that are key drivers of MASLD (4). For example, 17-beta hydroxysteroid dehydrogenase 13 (HSD17B13) is a novel lipid-droplet protein that has been identified from human steatotic liver biopsies (5). Three independent gene variants in *HSD17B13* which generate loss-of-function proteins are reported to associate with protection from liver injury (4, 6, 7). HSD17B13 gene expression and protein levels are upregulated in patients and mouse models of MASLD and overexpression of HSD17B13 in mice promotes rapid lipid accumulation in the liver of mice (5). However, the traditional gene knockout of *Hsd17b13* in mice had no beneficial effect on the development of liver steatosis with various dietary interventions (8). This surprising result suggests that the normal biological role of HSD17B13 and its metabolite pathway maybe important for normal liver function from birth, but abnormally elevated levels of HSD17B13 in adulthood is a pathological driver of steatotic liver.

In the present study, our analysis of unbiased, whole-genome RNA-sequencing in liver tissue from mice with high-fat diet (HFD) induced obesity and type-2 diabetes and mice treated with the synthetic retinoid Fenretinide to inhibit adiposity, insulin resistance and liver steatosis

84 (9, 10) revealed genes that are key drivers of MASLD including Hsd17b13. Thus, we
85 hypothesised that direct inhibition of elevated levels of liver HSD17B13 using RNAi-mediated
86 knockdown in vivo may reveal a beneficial phenotype and lead to novel insights into the
87 biological function of this uncharacterised lipid-droplet protein.

88 **MATERIALS AND METHODS**

89 **Animal studies**

90 All animal procedures were performed under a project license approved by the U.K. Home
91 Office under the Animals (Scientific Procedures) Act 1986 (PPL P1ECEB2B6) and the
92 University of Aberdeen Ethics Review Board. The Fenretinide HFD and *db/db* studies were
93 previously described (9, 10). For the Hsd17b13 knockdown study, 3-4 week male C57BL/6J mice
94 were purchased from Charles River. Mice were maintained at 22–24°C on 12-h light/dark cycle
95 with free access to food/water. At 11 weeks age, 18 mice were placed on to a 45% kcal HFD
96 (Research diets, D12451) whilst 8 remained on regular Chow. Following 21 weeks on HFD,
97 mice were randomised into two groups for intraperitoneal (i.p.) injection of AAV8-shscrmbl or
98 AAV8-shHsd17b13 (Vectorbuilder) at a virus titer of $1x10^{11}$ virus particles. Chow controls
99 received a saline injection of the same volume administered by i.p. injection. Body weight was
100 measured weekly and physiological tests performed. Two weeks (14 days) after virus-shRNA
101 injections, mice were killed (following 5 hours fasting) by CO2-induced anaesthesia and cervical
102 dislocation. Trunk blood following decapitation was collected and serum stored at -80°C. All
103 tissues were rapidly dissected, frozen in liquid nitrogen, and stored at -80°C. Tissues for
104 histology were fixed in formalin for 48h at 4°C, then stored at 4°C in phosphate-buffered saline
105 (PBS) until further processing.

106 **Physiological tests**

107 Body composition was measured before virus-shRNA injection to confirm HFD-induced obesity
108 and aid with randomization into treatment/control groups. The measurement was repeated 7 days
109 after shRNA treatment. Each mouse was analysed using an Echo MRI-3-in-1 scanner (Echo
110 Medical Systems, Houston, TX, USA). Glucose tolerance test (GTT) was performed at 10 days
111 post shRNA treatment. Briefly, mice were fasted for 5hrs, baseline glucose levels were sampled
112 from tail blood using glucose meters (AlphaTRAK, Abbott Laboratories, Abbot Park, IL, USA).

113 Subsequently mice were injected i.p. with 20% glucose (w/v) and blood glucose measured at 15,
114 30, 60 and 90 mins post-injection.

115 **Stable expression of HSD17B13 in cells**

116 HEK293 cells and HepG2, were maintained in Dulbecco's Modified Eagle Medium (DMEM)
117 GlutaMAX with 10% foetal bovine serum (FBS) at 37 ^{o}C and 5% CO_2. Human *HSD17B13*
118 (NCBI Accession number: NM_178135.5) with HA-tag on the C-terminus was cloned into
119 pcDNA3.1 (Genscript). HEK293 cells and HepG2 cells were transfected with HSD17B13 or
120 empty control vector using Lipofectamine 2000, cultured for 2-3 weeks in G418 for neomycin
121 resistance and positive colonies selected. Stable cell lines were treated with retinoic acid (RA, 1
122 µm, 2 h) or DMSO (vehicle control). Fatty acid (1mM 2:1 ratio of oleic and palmitic acid, 24 h)
123 or 1% methanol (vehicle control) was prepared with 10% bovine serum albumin (fatty acid free)
124 and 1% FBS in DMEM+G418.

125 **Immunoblotting**

126 Frozen liver tissues were homogenised in 400µl of ice-cold Radioimmunoprecipitation assay
127 buffer (10mM Tris-HCl pH 7.4, 150mM NaCl, 5mM EDTA pH 8.0, 1mM NaF, 0.1% SDS, 1%
128 Triton X-100, 1% Sodium Deoxycholate with freshly added 1mM $NaVO_4$ and protease
129 inhibitors) using a PowerGen 125 homogeniser and lysates normalised to 1µg/µl. Proteins were
130 separated on a 4-12% Bis-Tris gel (Fisher Scientific) by gel electrophoresis and transferred onto
131 a nitrocellulose membrane. Membranes were probed with the following primary antibodies:
132 HSD17B13 (1/500, ab122036, Abcam), GFP (1/1000, A11122, Invitrogen), GAPDH (1/1000,
133 14C10) and Vinculin (1/1000, 13901) both Cell Signaling Technology. Immunoblotting for RBP
134 (Dako) was from 1µl serum (11).

135 **RNA extraction and RT-qPCR**

136 Frozen tissues were lysed in TRIzol reagent (Sigma) and RNA isolated using phenol/chloroform
137 extraction according to manufacturer's instructions. RNA was then synthesized into cDNA
138 Tetrokit (Bioline, UK) and subjected to qPCR analysis using SYBR green and LightCycler 480
139 (Roche). Gene expression was determined relative to the reference gene *Nono* for mouse liver
140 tissue and *Hprt* for human cell lines (HEK and HepG2) and analysis was performed using the
141 Pfaffl method (12). Primer sequences can be found in Supplemental Table 1.

142

143 **Liver Histology**

144 Liver tissues were embedded in paraffin, sectioned and stained with haematoxylin and eosin
145 (H&E). Images were taken using a light microscope, EVOS XL (Thermofisher Scientfic, UK) at
146 20x and 40x magnification. Frozen liver tissue was used for fluorescent staining. Briefly,
147 processed slides were washed PBS for 10-12 min. Subsequently, slides were incubated with
148 Blocking (5% goat serum in PBS) and then with HCS Lipidtox^{TM} deep red neutral lipid stain
149 (H34477) (1:200 in PBS) in RT each for 1 h. Furthermore, they were mounted with fluoroshield
150 mounting medium with DAPI (ab104139).

151 **Liver and serum assays**

152 50-100mg of frozen liver tissues were homogenised in 1ml of PBS and frozen in liquid nitrogen
153 to enable further cell lysis. Samples were left to thaw at room temperature and centrifuged for
154 15s at 7500rpm to pellet debris. The remaining fat cake was resuspended in PBS, the resulting
155 supernatant used to determine total liver triglycerides according to manufacturer's instructions
156 (Sigma, cat: MAK266). Serum was analysed for alanine aminotransferase (ALT) activity
157 (Abcam, ab105134), FGF21 (R&D Systems, #MF2100) and total triglycerides (Sigma, cat:
158 MAK266) following manufacturer's guidelines.

159 **Lipidomics Analysis**

160 Global lipidomics analysis was performed by high resolution liquid chromatography-mass
161 spectrometry (LC-MS) using an Exactive Orbitrap mass spectrometer (Thermo Scientific, Hemel
162 Hempsted, UK) interfaced to a Thermo UltiMate 3000 RSLC system. Samples (10 µl) were
163 injected onto a Thermo Hypersil Gold C18 column (1.9 µm; 2.1 mm x 100 mm) maintained at
164 50°C. Mobile phase A consisted of water containing 10 mM ammonium formate and 0.1% (v/v)
165 formic acid. Mobile phase B consisted of a 90:10 mixture of isopropanol-acetonitrile containing
166 10 mM ammonium formate and 0.1% (v/v) formic acid. The initial conditions for analysis were
167 65%A-35%B, increasing to 65%B over 4 min and then to 100%B over 15 min, held for 2 min
168 prior to re-equilibration to the starting conditions over 6 min. The flow rate was 400 µl/min.
169 Analyses were undertaken in positive and negative ion modes at a resolution of 100,000 over the
170 mass-to-charge ratio (m/z) range of 250 to 2,000. Progenesis QI v3.0 (Nonlinear Dynamics,

171 Newcastle upon Tyne, UK) was used to process the data sets and lipids were identified through
172 interrogation of HMDB (http://www.hmdb.ca/), LIPID MAPS (www.lipidmaps.org/).
173 Multivariate statistical analysis was performed using SIMCA-P v13.0 (Umetrics, Umea,
174 Sweden) and the heatmap was generated with the online available platform MetaboAnalyst 5.0
175 (https://www.metaboanalyst.ca/) (13).

176 **RNA sequencing**

177 As previously described (10). Total RNA was extracted from frozen liver using TriZOL reagent
178 (Sigma Aldrich, Irvine, UK) to manufacturer's instructions. RNA was purified using RNeasy
179 miniprep kit (Qiagen, Manchester, UK) and quantified on a Bioanalyzer 2000 (Agilent
180 Technologies, Edinburgh, UK). Ribosomal RNA was removed from samples using the Ribo-
181 Zero rRNA removal kit (Illumina, San Diego, CA, USA). Sequencing libraries were prepared
182 using the TruSeq RNA Library Preparation Kit v2 (Illumina) following the low sample protocol,
183 using 1 μg RNA. Libraries were sequenced on the NextSeq-500 Desktop sequencer platform
184 (Illumina) with a 2 × 75 paired-end read length giving 719 million raw reads (average depth 45
185 million reads per sample). Reads were filtered using the FASTQ Toolkit v2.0.0 in the Illumina
186 BaseSpace cloud computing environment to remove adapter sequences and reads with phred
187 score <20 or length <20 bp. Filtered reads were checked using FastQC before aligning with
188 STAR 2.0 to the *Mus musculus* UCSC mm10 genome and differential expression measured using
189 DESeq2 with default parameters. RNA-seq data generated in this study has been deposited in the
190 NCBI Gene Expression Omnibus (GEO) database accession number GSE220684.

191 **Statistical Analysis.**

192 All values are expressed as mean + S.E.M, unless otherwise stated. Statistical analyses were
193 performed by using one- or two-way ANOVA (where stated) followed by multiple-comparison
194 tests to compare the means of three or more groups. In all figures, $*/^{\#}p \leq 0.05$, $**/^{\#\#}p \leq 0.01$,
195 $***/^{\#\#\#}p \leq 0.001$. All analyses were performed using GraphPad Prism (GraphPad Software).

196

197

198 **RESULTS**

199 **Hepatic RNA-seq reveals signature gene expression alterations in HFD-induced obese**
200 **steatotic liver and rescue by beneficial effects of Fenretinide**

201 We have previously reported the effects of Fenretinide to inhibit adiposity, insulin
202 resistance and the accumulation of liver triglycerides. To characterise the molecular mechanism
203 of beneficial effects of Fenretinide in the liver, we performed RNA-seq (GEO number
204 GSE220684) on liver tissue from HFD-induced obese C57BL/6 mice +/- Fenretinide for 20
205 weeks, compared to lean control mice (Figure 1A) (9, 10). HFD-induced obesity resulted in
206 upregulation of 941 liver genes and downregulation of 637 genes (Figure 1B). Many of the genes
207 upregulated in HFD steatotic liver were involved in triglyceride synthesis and fatty acid
208 metabolism and well-established targets of PPAR-alpha signalling and/or GWAS identified
209 genes associated with MASLD (e.g Hsd17b13, Figure 1C) (14). Fenretinide treatment prevented
210 the increase in expression of many of these genes (Figure 1C).

211 To further characterise the effects on gene expression changes linked to steatotic liver, we
212 compared the effects of Fenretinide on hepatic gene expression in HFD-induced and genetically
213 obese *db/db* mouse model (10). Both HFD and *db/db* obese mice had increased expression of
214 hepatic lipid metabolism genes (e.g. *Mogat* and *Crat*) (Figure 1D and 1E). Fenretinide treatment
215 prevented this increase in HFD mice but had no effect in *db/db* mice (Figure 1D and 1E).
216 Similarly, HFD repressed other genes (e.g. *Avpr1a* and *Hsd17b2*) and Fenretinide treatment
217 prevented this decrease in HFD mice but had no effect in *db/db* mice (Figure 1F and 1G). These
218 findings suggest the beneficial effects of Fenretinide treatment on hepatic gene expression are
219 associated with inhibition of HFD-induced adiposity and associated insulin resistance and
220 MASLD but not with genetically-obese *db/db* where adiposity and MASLD were not inhibited
221 by Fenretinide (9, 10).

222

223 **Hsd17b13 expression is upregulated in HFD-induced and genetic mouse models of obesity,**
224 **hyperglycaemia and MASLD.**

225 17β-Hydroxysteroid dehydrogenases (17β-HSDs) are a family of 15 members, which
226 play a key role in sex hormone metabolism by catalyzing steps of steroid biosynthesis (e.g.
227 Hsd17b1 and b2) (15, 16). Some may also play a role in cholesterol and fatty acid metabolism. Of
228 the hydroxysteroid 17-beta dehydrogenase family of genes the most closely related to *Hsd17b13*
229 is *Hsd17b11* although it is not specific to hepatocytes and also expressed in adipocytes (17).
230 HFD-induced obesity also upregulated *Hsd17b11 and Hsd17b7* hepatic gene expression in
231 C57BL/6 mice and Fenretinide treatment decreased their gene expression compared to HFD
232 mice (new Figure 2A RNA-seq mini-table Hsd17b family of genes). HFD also upregulated
233 *Hsd17b4* and *Hsd17b12* hepatic gene expression in C57BL/6 mice, however, Fenretinide
234 treatment had no effect to decrease these genes. *Hsd17b13* has been linked to MASLD and was
235 one of the top 10% most upregulated genes in C57BL/6 HFD mice, increased 1.5-fold (Figure
236 2A and 2B).

237 Hsd17b13 hepatic protein expression was also induced by a similar amount in HFD mice
238 compared to lean controls (Figure 2C). Fenretinide treatment was able to prevent this induction,
239 with both gene and protein expression levels close to lean C57BL/6 control mice (Figure 2A, 2B
240 and 2C). Fenretinide treatment also repressed Hsd17b13 expression in parallel with prevention of
241 liver steatosis in LDLR$^{-/-}$ mice fed-HFD plus high-cholesterol diet model of dyslipidemia
242 (Thompson et al., 2023 and Figure 2D) (18). *Hsd17b13* gene expression levels were induced in
243 two more genetical models of metabolic disease and steatotic liver, in leptin-deficient obese
244 *ob/ob* mice (Figure 2E) and in lipodystrophic Seipin/*Bscl2*$^{-/-}$ mice (Figure 2F) (19). FEN
245 treatment could not inhibit the increase in *Hsd17b13* obese *ob/ob* mice but gene therapy to
246 restore WAT in *Bscl2*$^{-/-}$ mice inhibited MASLD and *Hsd17b13* gene expression (Figure 2F) (20).
247 Taken together these data suggest a key role of 17β-Hydroxysteroid dehydrogenases and in
248 particular Hsd17b13 in MASLD.

249 **RNAi-mediated Hsd17b13 knockdown in HFD-induced obesity and MASLD does not**
250 **affect body weight, adiposity or glucose homeostasis**

251 To evaluate the role of Hsd17b13 in driving steatotic liver, we proceeded to directly
252 knockdown the elevated levels of this protein in adult mice with HFD-induced MASLD thereby

253 circumventing the lack of a protective effect of Hsd17b13 whole-body, total genetic knockout
254 from birth in mice. Candidate short hairpin RNA (shRNA) were tested for knockdown efficiency
255 in HEK293 cells overexpressing mouse *Hsd17b13*, and the most potent (hereafter renamed
256 shHsd17b13) was selected for treatment *in vivo*.

257 HFD caused increased weight gain and obesity over time compared to chow-fed
258 C57BL/6 mice, as expected (Figure 3A). At 21 weeks on HFD, obese mice were randomised for
259 administration of adeno-associated virus (AAV)-8 constructs encoding either shHsd17b13 or
260 scrambled control (shScrmbl) with the U6 promoter for high expression of shRNAs. shHsd17b13
261 treatment had no effect on body weight or adiposity compared to HFD-shscrmbl control in the
262 following 2 weeks (Figure 3B and C). Hepatic GFP co-expression confirmed successful AAV8
263 delivery in HFD mice (Figure 3D). shHsd17b13 treatment suppressed the elevated *Hsd17b13*
264 expression compared to shScrmbl treatment, normalising gene and protein expression to a level
265 similar to that in chow-fed lean mice (Figure 3E and F). HFD-induced obesity caused glucose
266 intolerance and shHsd17b13 knockdown had no effect to alter this compared to shScrmbl control
267 mice (Figure 3G, H and I).

268 **RNAi-mediated Hsd17b13 knockdown prevents HFD-induced MASLD and markers of**
269 **fibrotic injury.**

270 HFD-induced obesity and glucose intolerance led to steatotic liver characterised by
271 increased number and size of lipid droplets as determined by H&E staining of liver tissues and
272 fluorescent staining of lipid droplets (Figure 4A and B). Strikingly, *Hsd17b13* knockdown
273 substantially decreased the number and size of hepatic lipid droplets in HFD mice. In addition,
274 shHsd17b13 decreased liver triglycerides by 45% from the elevated level in HFD-shscrmbl and
275 back towards a normal level in CHOW mice (Figure 4C *first panel*). HFD-induced liver steatosis
276 was associated with elevated levels of serum ALT and serum Fgf21 compared to lean mice
277 (Figure 4C *second and third panels*). shHsd17b13 decreased both serum ALT levels and serum
278 Fgf21 indicating biomarkers of improved liver health compared to HFD-shscrmbl mice.

279 Persistent excess lipid accumulation and the progression to MASH, is associated with
280 activation of hepatic stellate cells by TGF-β which leads to the development of fibrosis by
281 collagens and matrix remodeling by tissue inhibitors of matrix metalloproteinases (21). HFD
282 increased the expression of *Col1a1*, *Timp1*, *Timp2*, *Tgf-β* (Figure 4D). Hsd17b13 knockdown

283 significantly decreased expression of *Timp2* and trended to decrease expression of *Col1a1*,
284 *Col4a1* and *Timp1, Tgf-β* in HFD mice. Similar changes in the pro-inflammatory macrophage
285 marker *Cd68* were determined. Thus, *Hsd17b13* knockdown and attenuation of excess hepatic
286 triglycerides storage, appeared to inhibit the development of fibrosis and MASH, via suppressing
287 gene expression alterations associated with hepatic stellate cell activation and a pro-
288 inflammatory environment.

289 **Increasing or decreasing Hsd17b13 levels does not affect retinoid transcriptional regulator**
290 **genes or serum RBP4.**

291 Hsd17b13 has been reported to have *in vitro* dehydrogenase activity towards retinol and thus
292 modulate retinoic acid levels in cells transfected with *Hsd17b13* (6). Thus, we determined
293 whether targets of retinoic acid signalling were altered with Hsd17b13 knockdown. HFD
294 increased hepatic *Lrat* expression which is associated with altered retinyl ester dynamics in
295 stellate cells and MASH (Figure 5A) (22, 23). Hsd17b13 knockdown trended to decrease
296 expression of *Lrat.* shHsd17b13 had no effect to alter the expression of nuclear receptors *Rara,*
297 *Rxra, Rxrb* or *Rarb,* a classic retinoic acid target gene (Figure 5A). HFD increased serum RBP4
298 levels in shScrmbl control mice compared to chow control and shHsd17b13 treatment had no
299 effect (Figure 5B). Our results suggest that Hsd17b13 does not modulate retinoic acid levels or
300 retinol homeostasis *in vivo*. To extend these studies further, we examined the effect of Hsd17b13
301 over-expression and retinoic acid in cells. Although retinoic acid could increase the expression of
302 *Cyp26a1* and *Rarb*, two classic retinoic acid inducible genes, Hsd17b13 over-expression had no
303 effect alone or in combination with retinoic acid to alter their gene expression (Figure 5C).
304 Hsd17b13 over-expression did increase *Raldh1* expression by >2-fold ($p<0.001$ by t-test) as did
305 retinoic acid treatment however there was no additive or synergistic interaction (by two-way
306 ANOVA). Our results suggest that Hsd17b13 does not play a significant role in modulating
307 retinoic acid levels or retinol homeostasis.

308 **Changing Hsd17b13 levels alters hepatic lipid and phospholipid metabolism.**

309 Dis-regulation of a network of hepatic genes involved in fatty acid metabolism in
310 response to over-nutrition contribute to excess hepatic lipid accumulation and thus MASLD. We
311 hypothesised that *Hsd17b13* knockdown mediated decrease in steatotic liver may be associated
312 with a rescue of this impairment. HFD increased hepatic expression of PPARα target genes

313 *Cd36*, *Vldlr, Crat* and *Mogat1* involved in fatty acid transport and metabolism, and shHsd17b13
314 treatment inhibited this induction (Figure 6A). To determine if these gene expression changes
315 were due to acute changes in HSD17B13 protein or linked secondarily to decreased hepatic lipid
316 accumulation next, we examined the effect of increased Hsd17b13 expression in cells. Increased
317 Hsd17b13 expression increased triglyceride storage in cells (Figure 6B) and increased *Cd36*
318 expression without additional fatty acids (Figure 6C). Fatty acid treatment further increased
319 triglyceride storage in cells with Hsd17b13 but did not change *Cd36* expression.

320 Next, we performed lipidomic analysis of liver tissues to understand the mechanism of
321 HSD17B13 biological function and role in MASFD. shHsd17b13 treatment decreased
322 diacylglycerols and increased phospholipids, in particular phosphatidylcholines containing
323 polyunsaturated fatty acids (PUFA) e.g. PC 34:3 and PC 42:10 (Figure 6D). We studied the
324 pathway which is responsible for the production of phospholipids and PUFAs. HFD increased
325 the expression of hepatic *Fads1* and *Lpcat3/Mboat5* (p=0.04 by t-test) and shHsd17b13
326 treatment did not significantly alter these (Figure 6E). HFD markedly increased hepatic *Cept1*
327 expression and shHsd17b13 treatment normalised *Cept1* expression in mice (Figure 6F). CEPT1
328 or Choline-enthanolamine phosphotransferase 1 catalyzes the terminal step of the Kennedy
329 pathway and is responsible for phosphatidylcholine (PC) and phosphatidylethanolamine (PE)
330 production (24). It is also reported to produce the endogenous ligand for PPAR-alpha, a
331 transcription factor that is a key regulator of hepatic lipid metabolism genes (25). Increased
332 Hsd17b13 expression in cells and increased *Cept1* expression -/+ additional fatty acids (Figure
333 6G). Thus, Hsd17b13 is a key driver of increased hepatic triglyceride storage and phospholipid
334 remodelling, likely via increased *Cept1* and *Cd36* expression, and may explain at least part of the
335 mechanism of it biological function and role in MASFD.

336

DISCUSSION

The multiple overlapping secondary pathologies in response to diet-induced obesity such as the development of type 2 diabetes, MASLD, atherosclerosis and CVD are a global medical burden. Currently there is no treatment for MASLD or MASH and thus therapies are urgently needed. We have previously reported the beneficial effects of Fenretinide to prevent the accumulation of hepatic triglycerides via decreased whole-body adiposity and associated insulin resistance. Here our RNA-seq study of liver tissue from HFD obese mice -/+ Fenretinide identified major beneficial effects of Fenretinide on hepatic gene expression including key drivers of MASLD e.g. HSD17B13. Thus, we sought to directly knockdown the elevated levels of Hsd17b13 to evaluate its role in driving MASLD and regulation of lipid/phospholipid metabolism.

HSD17B13 gene/protein expression are upregulated in MASLD and transgenic overexpression of HSD17B13 promotes rapid lipid accumulation in the liver of mice (5). However, the traditional gene knockout of HSD17B13 challenged with several diets to induce steatotic liver and/or fibrosis did not lead to the hypothesised protective phenotype (8). Our RNAi therapeutic approach, to suppress Hsd17b13 levels in adult mice with existing HFD-induced liver steatosis to decrease hepatic triglyceride storage is a translational approach to investigate the role of Hsd17b13 in MASLD. This RNAi knockdown strategy has been taken by pharma/biotech in on-going clinical trials (26). Possible explanations for the discrepancy between the phenotype of mouse genetic knockout and the RNAi knockdown approach, are if HSD17B13 affects other proteins in a mechanism independent of its enzymatic activity or total loss of Hsd17b13 activity is compensated for by another protein/pathway.

Su, Guan and co-workers (27) reported that Hsd17b13 interacts with ATGL on lipid droplets to regulate lipolysis in response to cAMP-PKA signalling, a mechanism that resembles a role played by Plin5 (28). Thereby, both Hsd17b13 and Plin5 have been shown to be phosphorylated leading to an increase in ATGL-mediated lipolysis. While this may be beneficial for MASLD, increased hepatic cAMP-PKA signalling is also associated with excess endogenous glucose production via gluconeogenesis in obesity and type 2 diabetes (29). Thus, it is not clear if this signalling network can be delineated sufficiently to facilitate targeting for the treatment of metabolic diseases. Recently, the X-ray crystal structure of Hsd17b13 has provided insights into a mechanism for association with the lipid droplet and interaction with ATGL or other potential

368 binding partners (30). The findings suggest that HSD17B13 may have an important scaffold
369 function at the lipid droplet.
370 Distinct changes occur in the liver lipidome with MASLD (31-33). Moreover, many genes
371 involved in hepatic PUFA and phospholipid metabolism, are important in the formation of
372 biologically important lipids and are linked to metabolic disease by human GWAS and mouse
373 knockout studies e.g. FADS1, ELOVL5, LPCAT3, MBOAT7, CEPT1, *PLA2G4A*/cPLA2α,
374 *PLA2G6*/iPLA2β, PTGDS and PTGES (34, 35) .The expression of these genes is also altered by
375 dysregulation of a network of transcription factors such as PPARa, LXR, SREBP. Our
376 lipidomics data suggests that HSD17B13 plays a key role in hepatic triglyceride and
377 phospholipid remodelling, whereby knockdown promoted an increase in phosphatidyl-cholines
378 (PC) containing PUFAs eg. PC 34:3 and PC 42:10. Studies of the human genetic variants of
379 Hsd17b13 (protective against severe liver disease) have reported an increase in phospholipids
380 including PC 34:3 (36). shHsd17b13 knockdown normalised liver *Cept1* expression in mice and
381 increased Hsd17b13 expression in cells led to increased *Cept1* expression. These results suggest
382 that Hsd17b13 may regulate phospholipid metabolism and may explain at least part of the
383 mechanism of it biological function and role in MASLD.
384 Several human genome-wide association studies have identified gene variants in
385 HSD17B13 which generate loss-of-function proteins that associate primarily with protection
386 from severity of MASLD and fibrosis i.e. progression to MASH (6, 7, 36-38). In agreement with
387 our *in vivo* data, mouse models have shown that inhibition/knockdown of Hsd17b13 protects
388 against both hepatic triglyceride accumulation and fibrosis (27, 39, 40) . We determined that
389 shHsd17b13 knockdown repressed hepatic fatty acid transporter Cd36 expression in mice and
390 reciprocally, increased Hsd17b13 expression in cells led to increased Cd36 expression.
391 Hepatocyte CD36 is a key factor in driving *de novo* lipogenesis and in the development of
392 MASLD (41-43). Thus, Hsd17b13 may play a role in the regulation of key transcription factors
393 (such as PPARa, LXR and SREBP) which coordinate the expression of hepatic lipid homeostasis
394 genes in response to physiological signals.
395 These data provide strong evidence for an important role of Hsd17b13 in driving
396 MASLD via regulation of hepatic triglyceride storage and phospholipid metabolism.
397 Importantly, this beneficial effect is present without an effect on body weight, adiposity or
398 glucose homeostasis suggesting that directly targeting Hsd17b13 is superior to the use of FEN,

399 which has diverse mechanisms of action. In addition, treating MASLD may prevent the
400 development of fibrosis/MASH and create an opportunity to clinically treat these without the
401 need to treat co-morbidities of obesity, type-2 diabetes and cardiovascular diseases. Thus, the
402 translation potential of targeting Hsd17b13 for MASLD/MASH is strong (26, 38).

403 **DATA AVAILABILITY**

404 Data will be made available upon reasonable request. Hepatic RNA-seq data generated in this
405 study (HFD+/-Fenretinide, 20 weeks in C57BL/6J mice) has been deposited in the NCBI Gene
406 Expression Omnibus (GEO) database accession number GSE220684.

407 **SUPPLEMENTAL MATERIAL**

408 Supplementary Table 1: qPCR Primers

409 **ACKNOWLEDGMENTS**

410 The authors thank the University of Aberdeen (UoA) animal research facility, qPCR core facility
411 (Institute of Medical Sciences, UoA) and Linda Davidson (NHS Grampian) for their technical
412 contributions regarding animal studies, qPCR and histology respectively. RNA-sequencing was
413 carried out at the UoA Centre for Genome Enabled Biology and Medicine (CGEBM); thanks to
414 Diane Stewart, Sophie Shaw and Elaina Collie-Duguid for support with sample prep,
415 bioinformatics reporting and project supervision. Thanks to Lars Grøntved (University of
416 Southern Denmark) for invaluable discussions about the RNA-seq bioinformatic analysis.
417 Lipidomics was performed at Glasgow Polyomics (University of Glasgow). The authors also
418 wish to thank Mirela Delibegovic (UoA) for invaluable discussions throughout the study and
419 review of the manuscript and members of the Delibegovic-Mody joint lab for their technical
420 contributions.

421 **GRANTS**

422 This study was supported by a James Mearns Trust PhD studentship (to S. Mahmood); British
423 Heart Foundation (PG16/90/32518) project grant and Wellcome Trust ISSF small project grant
424 (to N. Mody) and Wellcome Trust ISSF international partnership award (to N. Mody and Lars
425 Grøntved, University of Southern Denmark); UoA CGEBM PhD studentship (to N. Morrice).

426 **DISCLOSURES**

427 None

428 ## DISCLAIMERS

429 None

430 ## AUTHOR CONTRIBUTIONS

431 GM and N.Mody conceived and designed research; S.Mahmood, N. Morrice, DT, S.
432 Milanizadeh, SW and PW performed experiments and analyzed data; JR and N.Mody interpreted
433 results of experiments; S.Mahmood, S. Milanizadeh, SW, DT and PW prepared figures;
434 S.Mahmood drafted the manuscript and N.Mody edited and revised the manuscript, S.Mahmood,
435 N. Morrice, GM and N.Mody approved final version of manuscript.

436 ## REFERENCES

437 1. Pafili K, Roden M: Nonalcoholic fatty liver disease (NAFLD) from pathogenesis to treatment
438 concepts in humans. *Mol Metab.* 50:101122, 2021

439 2. Luo Q, Wei R, Cai Y, Zhao Q, Liu Y, Liu WJ: Efficacy of off-label therapy for non-alcoholic
440 fatty liver disease in improving non-invasive and invasive biomarkers: A systematic review and
441 network meta-analysis of randomized controlled trials. *Front Med (Lausanne).* 9:793203, 2022

442 3. Esler WP, Bence KK: Metabolic targets in nonalcoholic fatty liver disease. *Cell Mol*
443 *Gastroenterol Hepatol.* 8:247-267, 2019

444 4. Chella Krishnan K, Kurt Z, Barrere-Cain R, Sabir S, Das A, Floyd R, Vergnes L, Zhao Y, Che
445 N, Charugundla S, Qi H, Zhou Z, Meng Y, Pan C, Seldin MM, Norheim F, Hui S, Reue K, Lusis
446 AJ, Yang X: Integration of multi-omics data from mouse diversity panel highlights
447 mitochondrial dysfunction in non-alcoholic fatty liver disease. *Cell Syst.* 6:103-115.e7, 2018

448 5. Su W, Wang Y, Jia X, Wu W, Li L, Tian X, Li S, Wang C, Xu H, Cao J, Han Q, Xu S, Chen
449 Y, Zhong Y, Zhang X, Liu P, Gustafsson JA, Guan Y: Comparative proteomic study reveals
450 17beta-HSD13 as a pathogenic protein in nonalcoholic fatty liver disease. *Proc Natl Acad Sci U*
451 *S A.* 111:11437-11442, 2014

452 6. Ma Y, Belyaeva OV, Brown PM, Fujita K, Valles K, Karki S, de Boer YS, Koh C, Chen Y,
453 Du X, Handelman SK, Chen V, Speliotes EK, Nestlerode C, Thomas E, Kleiner DE, Zmuda JM,

454 Sanyal AJ, (for the Nonalcoholic Steatohepatitis Clinical Research Network), Kedishvili NY,
455 Liang TJ, Rotman Y: 17-beta hydroxysteroid dehydrogenase 13 is a hepatic retinol
456 dehydrogenase associated with histological features of nonalcoholic fatty liver disease.
457 *Hepatology.* 69:1504-1519, 2019

458 7. Abul-Husn NS, Cheng X, Li AH, Xin Y, Schurmann C, Stevis P, Liu Y, Kozlitina J, Stender
459 S, Wood GC, Stepanchick AN, Still MD, McCarthy S, O'Dushlaine C, Packer JS,
460 Balasubramanian S, Gosalia N, Esopi D, Kim SY, Mukherjee S, Lopez AE, Fuller ED, Penn J,
461 Chu X, Luo JZ, Mirshahi UL, Carey DJ, Still CD, Feldman MD, Small A, Damrauer SM, Rader
462 DJ, Zambrowicz B, Olson W, Murphy AJ, Borecki IB, Shuldiner AR, Reid JG, Overton JD,
463 Yancopoulos GD, Hobbs HH, Cohen JC, Gottesman O, Teslovich TM, Baras A, Mirshahi T,
464 Gromada J, Dewey FE: A protein-truncating HSD17B13 variant and protection from chronic
465 liver disease. *N Engl J Med.* 378:1096-1106, 2018

466 8. Ma Y, Brown PM, Lin DD, Ma J, Feng D, Belyaeva OV, Podszun MC, Roszik J, Allen JN,
467 Umarova R, Kleiner DE, Kedishvili NY, Gavrilova O, Gao B, Rotman Y: 17-beta
468 hydroxysteroid dehydrogenase 13 deficiency does not protect mice from obesogenic diet injury.
469 *Hepatology.* 73:1701-1716, 2021

470 9. Mcilroy GD, Delibegovic M, Owen C, Stoney PN, Shearer KD, McCaffery PJ, Mody N:
471 Fenretinide treatment prevents diet-induced obesity in association with major alterations in
472 retinoid homeostatic gene expression in adipose, liver, and hypothalamus. *Diabetes.* 62:825-836,
473 2013

474 10. Morrice N, Mcilroy GD, Tammireddy SR, Reekie J, Shearer KD, Doherty MK, Delibegovic
475 M, Whitfield PD, Mody N: Elevated fibroblast growth factor 21 (FGF21) in obese, insulin
476 resistant states is normalised by the synthetic retinoid fenretinide in mice. *Sci Rep.* 7:43782, 2017

477 11. Yang Q, Graham TE, Mody N, Preitner F, Peroni OD, Zabolotny JM, Kotani K, Quadro L,
478 Kahn BB: Serum retinol binding protein 4 contributes to insulin resistance in obesity and type 2
479 diabetes. *Nature.* 436:356-62, 2005

480 12. Pfaffl MW: A new mathematical model for relative quantification in real-time RT-PCR.
481 *Nucleic Acids Res.* 29:e45, 2001

482 13. Pang Z, Chong J, Zhou G, de Lima Morais DA, Chang L, Barrette M, Gauthier C, Jacques P,
483 Li S, Xia J: MetaboAnalyst 5.0: Narrowing the gap between raw spectra and functional insights.
484 *Nucleic Acids Res.* 49:W388-W396, 2021

485 14. Kersten S: Integrated physiology and systems biology of PPARalpha. *Mol Metab.* 3:354-371,
486 2014

487 15. Poutanen M, Penning TM: Biology and clinical relevance of hydroxysteroid (17beta)
488 dehydrogenase enzymes. *Mol Cell Endocrinol.* 489:1-2, 2019

489 16. Marchais-Oberwinkler S, Henn C, Moller G, Klein T, Negri M, Oster A, Spadaro A, Werth
490 R, Wetzel M, Xu K, Frotscher M, Hartmann RW, Adamski J: 17beta-hydroxysteroid
491 dehydrogenases (17beta-HSDs) as therapeutic targets: Protein structures, functions, and recent
492 progress in inhibitor development. *J Steroid Biochem Mol Biol.* 125:66-82, 2011

493 17. Horiguchi Y, Araki M, Motojima K: 17beta-hydroxysteroid dehydrogenase type 13 is a liver-
494 specific lipid droplet-associated protein. *Biochem Biophys Res Commun.* 370:235-238, 2008

495 18. Thompson D, Mahmood S, Morrice N, Kamli-Salino S, Dekeryte R, Hoffmann PA, Doherty
496 MK, Whitfield PD, Delibegovic M, Mody N: Fenretinide inhibits obesity and fatty liver disease
497 but induces Smpd3 to increase serum ceramides and worsen atherosclerosis in LDLR(-/-) mice.
498 *Sci Rep.* 13:3937-w, 2023

499 19. Mcilroy GD, Suchacki K, Roelofs AJ, Yang W, Fu Y, Bai B, Wallace RJ, De Bari C,
500 Cawthorn WP, Han W, Delibegovic M, Rochford JJ: Adipose specific disruption of seipin causes
501 early-onset generalised lipodystrophy and altered fuel utilisation without severe metabolic
502 disease. *Mol Metab.* 10:55-65, 2018

503 20. Sommer N, Roumane A, Han W, Delibegovic M, Rochford JJ, Mcilroy GD: Gene therapy
504 restores adipose tissue and metabolic health in a pre-clinical mouse model of lipodystrophy. *Mol*
505 *Ther Methods Clin Dev.* 27:206-216, 2022

506 21. Friedman SL, Neuschwander-Tetri BA, Rinella M, Sanyal AJ: Mechanisms of NAFLD
507 development and therapeutic strategies. *Nat Med.* 24:908-922, 2018

508 22. Molenaar MR, Penning LC, Helms JB: Playing jekyll and hyde-the dual role of lipids in fatty
509 liver disease. *Cells.* 9:2244. doi: 10.3390/cells9102244, 2020

510 23. Saeed A, Dullaart RPF, Schreuder TCMA, Blokzijl H, Faber KN: Disturbed vitamin A
511 metabolism in non-alcoholic fatty liver disease (NAFLD). *Nutrients.* 10:29. doi:
512 10.3390/nu10010029, 2017

513 24. Gibellini F, Smith TK: The kennedy pathway--de novo synthesis of
514 phosphatidylethanolamine and phosphatidylcholine. *IUBMB Life.* 62:414-428, 2010

515 25. Chakravarthy MV, Lodhi IJ, Yin L, Malapaka RRV, Xu HE, Turk J, Semenkovich CF:
516 Identification of a physiologically relevant endogenous ligand for PPARalpha in liver. *Cell.*
517 138:476-488, 2009

518 26. Amangurbanova M, Huang DQ, Loomba R: Review article: The role of HSD17B13 on
519 global epidemiology, natural history, pathogenesis and treatment of NAFLD. *Aliment Pharmacol*
520 *Ther.* 57:37-51, 2023

521 27. Su W, Wu S, Yang Y, Guo Y, Zhang H, Su J, Chen L, Mao Z, Lan R, Cao R, Wang C, Xu H,
522 Zhang C, Li S, Gao M, Chen X, Zheng Z, Wang B, Liu Y, Liu Z, Wang Z, Liu B, Fan X, Zhang
523 X, Guan Y: Phosphorylation of 17beta-hydroxysteroid dehydrogenase 13 at serine 33 attenuates
524 nonalcoholic fatty liver disease in mice. *Nat Commun.* 13:6577-1, 2022

525 28. Keenan SN, De Nardo W, Lou J, Schittenhelm RB, Montgomery MK, Granneman JG, Hinde
526 E, Watt MJ: Perilipin 5 S155 phosphorylation by PKA is required for the control of hepatic lipid
527 metabolism and glycemic control. *J Lipid Res.* 62:100016, 2021

528 29. Yang H, Yang L: Targeting cAMP/PKA pathway for glycemic control and type 2 diabetes
529 therapy. *J Mol Endocrinol.* 57:R93-R108, 2016

530 30. Liu S, Sommese RF, Nedoma NL, Stevens LM, Dutra JK, Zhang L, Edmonds DJ, Wang Y,
531 Garnsey M, Clasquin MF: Structural basis of lipid-droplet localization of 17-beta-hydroxysteroid
532 dehydrogenase 13. *Nat Commun.* 14:5158-0, 2023

533 31. McGlinchey AJ, Govaere O, Geng D, Ratziu V, Allison M, Bousier J, Petta S, de Oliviera C,
534 Bugianesi E, Schattenberg JM, Daly AK, Hyotylainen T, Anstee QM, Oresic M: Metabolic
535 signatures across the full spectrum of non-alcoholic fatty liver disease. *JHEP Rep.* 4:100477,
536 2022

537 32. Ooi GJ, Meikle PJ, Huynh K, Earnest A, Roberts SK, Kemp W, Parker BL, Brown W,
538 Burton P, Watt MJ: Hepatic lipidomic remodeling in severe obesity manifests with steatosis and
539 does not evolve with non-alcoholic steatohepatitis. *J Hepatol.* 75:524-535, 2021

540 33. Velenosi TJ, Ben-Yakov G, Podszun MC, Hercun J, Etzion O, Yang S, Nadal C, Haynes-
541 Williams V, Huang WA, Gonzalez-Hodar L, Brychta RJ, Takahashi S, Akkaraju V, Krausz KW,
542 Walter M, Cai H, Walter PJ, Muniyappa R, Chen KY, Gonzalez FJ, Rotman Y: Postprandial
543 plasma lipidomics reveal specific alteration of hepatic-derived diacylglycerols in nonalcoholic
544 fatty liver disease. *Gastroenterology.* 162:1990-2003, 2022

545 34. Zhang JY, Kothapalli KSD, Brenna JT: Desaturase and elongase-limiting endogenous long-
546 chain polyunsaturated fatty acid biosynthesis. *Curr Opin Clin Nutr Metab Care.* 19:103-110,
547 2016

548 35. Jalil A, Bourgeois T, Menegaut L, Lagrost L, Thomas C, Masson D: Revisiting the role of
549 LXRs in PUFA metabolism and phospholipid homeostasis. *Int J Mol Sci.* 20:3787. doi:
550 10.3390/ijms20153787, 2019

551 36. Luukkonen PK, Tukiainen T, Juuti A, Sammalkorpi H, Haridas PAN, Niemela O, Arola J,
552 Orho-Melander M, Hakkarainen A, Kovanen PT, Dwivedi O, Groop L, Hodson L, Gastaldelli A,
553 Hyotylainen T, Oresic M, Yki-Jarvinen H: Hydroxysteroid 17-beta dehydrogenase 13 variant
554 increases phospholipids and protects against fibrosis in nonalcoholic fatty liver disease. *JCI*
555 *Insight.* 5:e132158. doi: 10.1172/jci.insight.132158, 2020

556 37. Anstee QM, Darlay R, Cockell S, Meroni M, Govaere O, Tiniakos D, Burt AD, Bedossa P,
557 Palmer J, Liu Y, Aithal GP, Allison M, Yki-Jarvinen H, Vacca M, Dufour J, Invernizzi P, Prati
558 D, Ekstedt M, Kechagias S, Francque S, Petta S, Bugianesi E, Clement K, Ratziu V,
559 Schattenberg JM, Valenti L, Day CP, Cordell HJ, Daly AK, EPoS Consortium Investigators:
560 Genome-wide association study of non-alcoholic fatty liver and steatohepatitis in a histologically
561 characterised cohort(☆). *J Hepatol.* 73:505-515, 2020

562 38. Zhang H, Su W, Xu H, Zhang X, Guan Y: HSD17B13: A potential therapeutic target for
563 NAFLD. *Front Mol Biosci.* 8:824776, 2022

564 39. Wang M, Li J, Li H, Dong B, Jiang J, Liu N, Tan J, Wang X, Lei L, Li H, Sun H, Tang M,
565 Wang H, Yan H, Li Y, Jiang J, Peng Z: Down-regulating the high level of 17-beta-
566 hydroxysteroid dehydrogenase 13 plays a therapeutic role for non-alcoholic fatty liver disease.
567 *Int J Mol Sci.* 23:5544. doi: 10.3390/ijms23105544, 2022

568 40. Luukkonen PK, Sakuma I, Gaspar RC, Mooring M, Nasiri A, Kahn M, Zhang X, Zhang D,
569 Sammalkorpi H, Penttila AK, Orho-Melander M, Arola J, Juuti A, Zhang X, Yimlamai D, Yki-
570 Jarvinen H, Petersen KF, Shulman GI: Inhibition of HSD17B13 protects against liver fibrosis by
571 inhibition of pyrimidine catabolism in nonalcoholic steatohepatitis. *Proc Natl Acad Sci U S A.*
572 120:e2217543120, 2023

573 41. Koonen DPY, Jacobs RL, Febbraio M, Young ME, Soltys CM, Ong H, Vance DE, Dyck
574 JRB: Increased hepatic CD36 expression contributes to dyslipidemia associated with diet-
575 induced obesity. *Diabetes.* 56:2863-2871, 2007

576 42. Wilson CG, Tran JL, Erion DM, Vera NB, Febbraio M, Weiss EJ: Hepatocyte-specific
577 disruption of CD36 attenuates fatty liver and improves insulin sensitivity in HFD-fed mice.
578 *Endocrinology.* 157:570-585, 2016

579 43. Rada P, Gonzalez-Rodriguez A, Garcia-Monzon C, Valverde AM: Understanding
580 lipotoxicity in NAFLD pathogenesis: Is CD36 a key driver? *Cell Death Dis.* 11:802-w, 2020

581

582

583 # FIGURE LEGENDS

584

585 **Figure 1**: **Hepatic gene expression in high-fat diet-induced obese and genetically-obese mice**
586 **with liver steatosis, and effects of Fenretinide treatment.**

587 **A**. Graphical illustration of mouse liver study described.

588 **B**. Volcano plot of hepatic RNA-seq data of HFD (obese-steatotic liver) most highly induced
589 genes by fold change and significance, compared to lean control mice (10).

590 **C**. Shortlist of differential gene expression from RNA-seq data, reciprocally regulated genes in
591 HFD (obese-steatotic liver) +/-FEN, involved in triglyceride synthesis and fatty acid metabolism
592 and genes associated with MASLD. HFD induced genes vs lean control mice and FEN-HFD
593 repressed genes vs HFD, significance, adjusted p-value *** $<10^{-15}$, ** $<10^{-8}$, * $<10^{-3}$, ns not
594 significant.

595 **D**. and **F**. Hepatic gene expression in HFD (obese-steatotic liver) mice +/-FEN.

596 **E**. and **G**. Hepatic gene expression in *db/db* (genetically-obese steatotic liver) mice +/- FEN.

597 Data (n=7-8 per group) are presented as mean + SEM and analysed by one-way ANOVA
598 followed by Bonferroni multiple comparison tests where *$p \leq 0.05$, **$p \leq 0.01$ and ***$p \leq 0.001$
599 (HFD vs CHOW and *db/db* vs lean) or # $p \leq 0.05$ and ## $p \leq 0.01$ and ### $p \leq 0.001$ (FEN-HFD vs
600 HFD and FEN-*db/db* vs *db/db*).

601

602

603 **Figure 2**: **<u>Increased Hsd17b13 expression in a HFD-induced and genetic mouse models of</u>**
604 **<u>obesity, hyperglycaemia and MASLD.</u>**

605 **A**. Differential gene expression from RNA-seq data. Hydroxysteroid 17-beta dehydrogenase
606 family of genes reciprocally regulated in HFD (obese-steatotic liver) +/-FEN. HFD induced
607 genes vs lean control mice and FEN-HFD repressed genes vs HFD, significance, adjusted p-
608 value *** $<10^{-15}$, ** $<10^{-8}$, * $<10^{-3}$, ns not significant.

609 **B**. *Hsd17b13* gene expression in HFD (obese-steatotic liver) mice +/-FEN and chow fed lean
610 controls, normalised to *Nono*, (n=7-8 per group).

611 **C**. Western blot of Hsd17b13 protein expression in HFD (obese-steatotic liver) mice +/-FEN and
612 chow fed lean controls, and quantification normalised to Gapdh, (n=4 per group).

613 **D**. Western blot and quantification of HSD17B13 protein expression in *Ldlr*$^{-/-}$ HFD (obese-
614 steatotic liver) mice +/-FEN and control (10% kcal) fat diet lean controls, and quantification
615 normalised to vinculin, (n=5-6 per group).

616 **E**. *Hsd17b13* gene expression in *ob/ob* (genetically-obese steatotic liver) mice +/-FEN and
617 control (10% kcal) fat diet lean controls, normalised to *Nono*, (n=6-7 per group).

618 **F**. *Hsd17b13* gene expression in *Bscl2*$^{-/-}$ (lipodystrophic steatotic liver) mice +/- human *Bscl2*$^{-/-}$
619 rescue and wildtype control, normalised to *Nono*, (n=8-9 per *Bscl2*$^{-/-}$ groups, n=11 wildtype
620 control).

621 Data are presented as mean + SEM and analysed by one-way ANOVA followed by Bonferroni
622 multiple comparison tests where *$p \leq 0.05$, **$p \leq 0.01$ and ***$p \leq 0.001$ (respective MASLD model
623 vs control) or ## $p \leq 0.01$ (FEN-HFD vs HFD).

624

625

626

627 **Figure 3: <u>Effect of RNAi-mediated Hsd17b13 knockdown on HFD-induced obesity and</u>**
628 **<u>glucose homeostasis</u>**

629 **A**. Body weights of C57BL/6 mice on high-fat diet (HFD, 45% kCal fat) or control CHOW diet
630 for 23 weeks. At 21 weeks on HFD, obese mice were randomised for administration of AAV8-
631 GFP-shHsd17b13 or scrambled control shRNA (shScrmbl), n=8-9 per group.

632 **B**. Change in body weight from 21 to 23 weeks diet and

633 **C**. Adiposity (% body fat) at week 22 HFD in response to administration of AAV8-GFP-shRNA.

634 At 23 weeks, following administration of AAV8-GFP-shHsd17b13 or shScrmbl,

635 **D**. Western blot of GFP in representative mouse liver tissues

636 **E**. *Hsd17b13* gene expression in mouse livers, n=8 per group

637 **F**. Western blot of Hsd17b13 protein expression and vinculin (loading control) in mouse livers
638 and quantification, n=4-5 per group.

639 **G**. Fasting (5 hours) glycaemia (basal glycemia from GTT). *$p \leq 0.05$ (shHsd17b13 HFD vs
640 Chow)

641 **H**. Glucose tolerance test (GTT) performed in week 2 post-treatment with shHsd17b13 or
642 shScrmbl, n=8-9 per group,

643 **I**. Area under curve (AUC) from GTT for each individual mouse.

644 All data presented as mean ± SEM and analysed by one-way ANOVA followed by Bonferroni
645 multiple comparison tests where

646 *$p \leq 0.05$, **$p \leq 0.01$ and ***$p \leq 0.001$ (HFD groups vs Chow)

647 #$p \leq 0.05$ and ### $p \leq 0.001$ (HFD- shHsd17b13 vs HFD-shscrmbl)

648 In addition, in **F**. Western blot quantification, One-way ANOVA #$p \leq 0.05$ (HFD- shHsd17b13 vs
649 HFD-shscrmbl) but required t-test for *$p \leq 0.05$, (HFD-shscrmbl vs Chow).

650 in **H**. GTT, t-tests were performed at individual time-points and where ### $p \leq 0.001$ (HFD-
651 shHsd17b13 vs Chow).

652 **Figure 4**: **<u>Effect of RNAi-mediated Hsd17b13 knockdown on HFD-induced MASLD</u>**.

653 **A**. H&E staining of representative liver tissues at 20x and 40x magnification and

654 **B**. fluorescent staining of lipid droplets

655 in C57BL/6 control CHOW diet mice or HFD obese mice treated with shHsd17b13 or scrambled
656 control (shScrmbl).

657 Scale bars are 200 µm (20x) and 100 µm (40x) in H&E images and 20 µm in fluorescent images
658 respectively.

659 **C**. Liver triglyceride levels, serum ALT activity and serum FGF21 levels.

660 **D.** Gene expression of fibrosis markers in liver tissue, Collagen type I alpha 1 (*Col1a1*),
661 Collagen type IV alpha 1 (*Col4a1*), Tissue inhibitor of metalloproteinases (*Timp*)-*1* and *Timp2*,
662 Transforming growth factor beta (*Tgf-β*)-1 and Cluster of Differentiation (*Cd*)-*68*.

663 Data in **C**) and **D**) are presented as mean ± SEM (n=8 per group) and analysed by one-way
664 ANOVA followed by Bonferroni multiple comparison tests where * $p \leq 0.05$, ** $p \leq 0.01$ and
665 *** $p \leq 0.001$ (comparing HFD groups to control CHOW diet) or # $p \leq 0.05$ and ## $p \leq 0.01$
666 (comparing HFD-shHsd17b13 to HFD-shscrmbl).

667

668 **Figure 5**: **<u>Effect of altered Hsd17b13 levels on retinoid genes and serum RBP4.</u>**

669 **A**. Gene expression of hepatic lecithin-retinol acyltransferase (*Lrat*) and *Retinoic Acid* and
670 *Retinoid X receptors* (*Rar* and *Rxr*) transcription factors (n=8 per group)

671 in C57BL/6 control CHOW diet mice or HFD obese mice treated with shHsd17b13 or scrambled
672 control (shScrmbl).

673 **B**. Western blot and quantification of serum RBP4 levels (n=5-6 per group).

674 Data is presented as mean ± SEM with analysed by One-way ANOVA (*$p \leq 0.05$) followed by
675 Bonferroni multiple comparison tests where * $p \leq 0.05$ and ** $p \leq 0.01$ (comparing HFD groups to
676 control CHOW diet).

677 **C**. HEK293 cells were transfected with HA-tagged Hsd17b13 or pcDNA3.1 control plasmid to
678 stably express Hsd17b13 and treated with retinoic acid (RA, 1 µm, 2 h) or DMSO (vehicle
679 control).

680 Gene expression of *Hsd17b13* and retinoic acid metabolism genes *Cyp26a1*, *Raldh1* and *Rarb.*

681 Data is presented as mean ± SEM from n=3 biological replicates and analysed by two-way
682 ANOVA where *** $p \leq 0.001$ (Hsd17b13 cells vs pcDNA control cells), # $p \leq 0.05$ and ## $p \leq 0.01$
683 and ### $p \leq 0.001$ (RA vs DMSO control). Hsd17b13 over-expression did increase *Raldh1*
684 expression by >2-fold ($p < 0.001$ by t-test)

685

686

687 **Figure 6**: **<u>Effect of altered Hsd17b13 levels on lipid and phospholipid metabolism</u>**

688 **A**. Gene expression of hepatic lipid metabolism genes (n=8 per group)

689 in C57BL/6 control CHOW diet mice or HFD obese mice treated with shHsd17b13 or scrambled
690 shRNA (shScrmbl).

691 **B**. HepG2 cells stably expressing HA-tagged Hsd17b13 or pcDNA3.1 control plasmid were
692 treated with 1mM fatty acid (2:1 ratio of oleic and palmitic acid) or methanol (vehicle control).
693 Cells were stained with oil red O. Images are representative of 24 hour treatment. Scale bar =
694 100μM.

695 **C**. Fatty acid translocase *Cd36* gene expression HEK293 cells expressing Hsd17b13 or
696 pcDNA3.1 control and treated with 1mM fatty acid (2:1 ratio of oleic and palmitic acid) or
697 methanol (vehicle control).

698 **D**. Lipidomic analysis heatmap of most significant ($p<0.05$) changes in lipids, enriched in
699 diacylglycerides and phospholipid species in liver tissue from C57BL/6 HFD obese mice treated
700 with shHsd17b13 or scrambled shRNA (shScrmbl), n=3 for each.

701 **E**. and **F**. Gene expression of key regulators of phospholipid metabolism (n=8 per group)

702 **G**. *Cept1* (Choline-enthanolamine phosphotransferase 1) gene expression HEK293 cells
703 expressing Hsd17b13 or pcDNA3.1 control and treated with 1mM fatty acid (2:1 ratio of oleic
704 and palmitic acid) or methanol (vehicle control).

705 All data is presented as mean ± SEM.

706 **A**., **E**. and **F**. were analysed by one-way ANOVA followed by Bonferroni multiple comparison
707 tests where * $p\leq0.05$, ** $p\leq0.01$ and *** $p\leq0.001$ (HFD groups vs CHOW diet) or # $p\leq0.05$, ##
708 $p\leq0.01$ and ### $p\leq0.001$ (shHsd17b13 vs shscrmbl). Fads1 and Lpcat3 were increased in HFD,
709 $p\leq0.05$ by t-test.

710 **C**. and **G**. were analysed by two-way ANOVA

711 where * $p\leq0.05$ and *** $p\leq0.001$ (Hsd17b13 cells vs pcDNA control cells), # $p\leq0.05$ and ##
712 $p\leq0.01$ and ### $p\leq0.001$ (fatty acid vs methanol control).

FIGURE 1

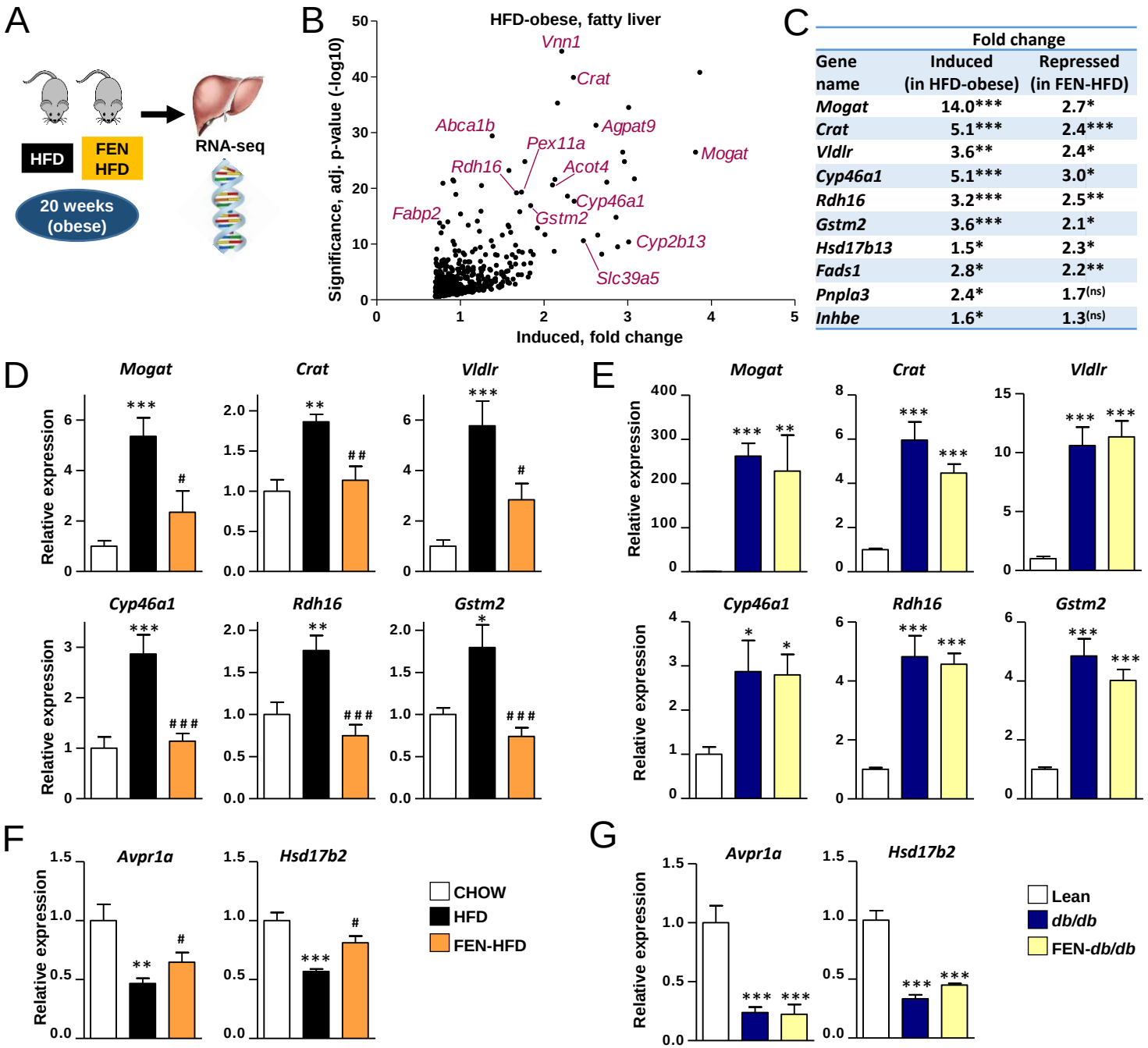

Gene name	Fold change: Induced (in HFD-obese)	Fold change: Repressed (in FEN-HFD)
Mogat	14.0***	2.7*
Crat	5.1***	2.4***
Vldlr	3.6**	2.4*
Cyp46a1	5.1***	3.0*
Rdh16	3.2***	2.5**
Gstm2	3.6***	2.1*
Hsd17b13	1.5*	2.3*
Fads1	2.8*	2.2**
Pnpla3	2.4*	1.7(ns)
Inhbe	1.6*	1.3(ns)

FIGURE 2

A

Gene name	Fold change Induced (in HFD-obese)	Fold change Repressed (in FEN-HFD)
Hsd17b7	1.78 **	-1.57 *
Hsd17b13	1.54 *	-2.28 ***
Hsd17b12	1.53 ***	-1.29 ns
Hsd17b4	1.47 ***	-1.28 ns
Hsd17b11	1.21 *	-1.33 **

B

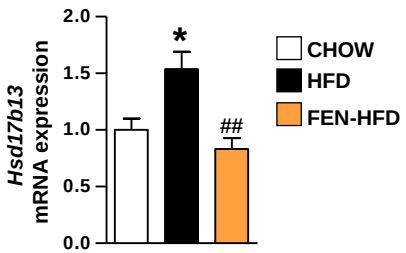

C

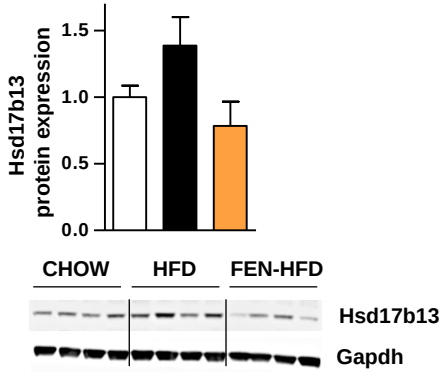

D

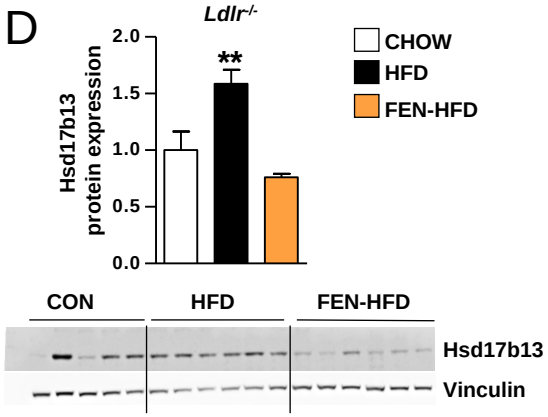

E

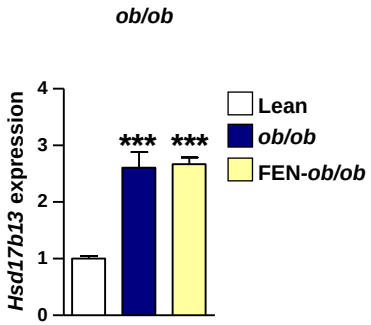

F

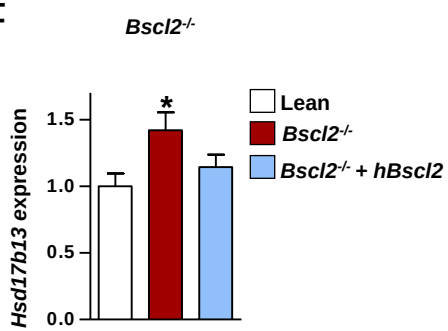

FIGURE 3

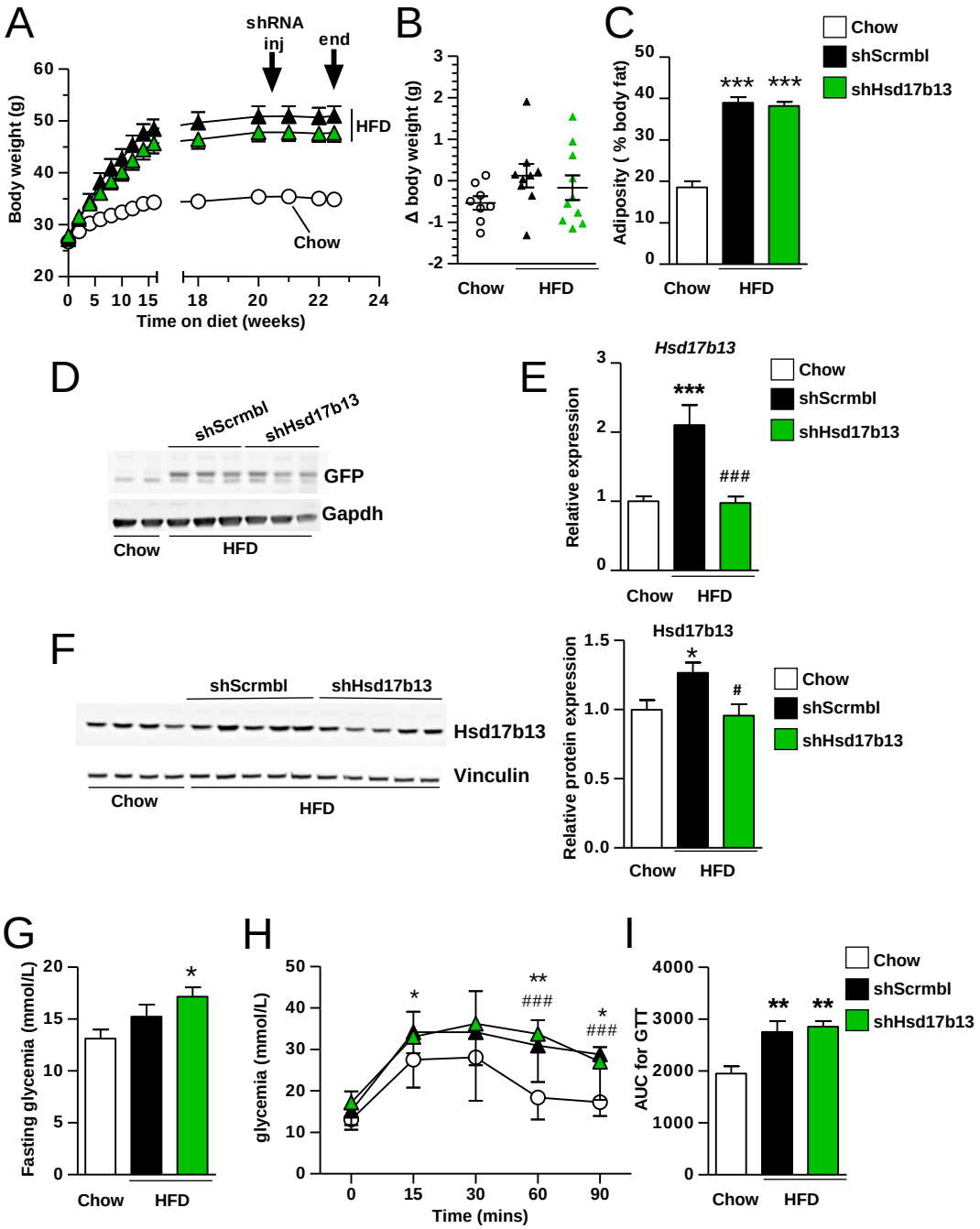
A
shRNA inj
end
Body weight (g)
HFD
Chow
Time on diet (weeks)
B
Δ body weight (g)
Chow
HFD
C
Adiposity (% body fat)
Chow
shScrmbl
shHsd17b13
D
shScrmbl
shHsd17b13
GFP
Gapdh
Chow
HFD
E
Hsd17b13
Relative expression
F
shScrmbl
shHsd17b13
Hsd17b13
Vinculin
Relative protein expression
G
Fasting glycemia (mmol/L)
H
glycemia (mmol/L)
Time (mins)
I
AUC for GTT

FIGURE 4

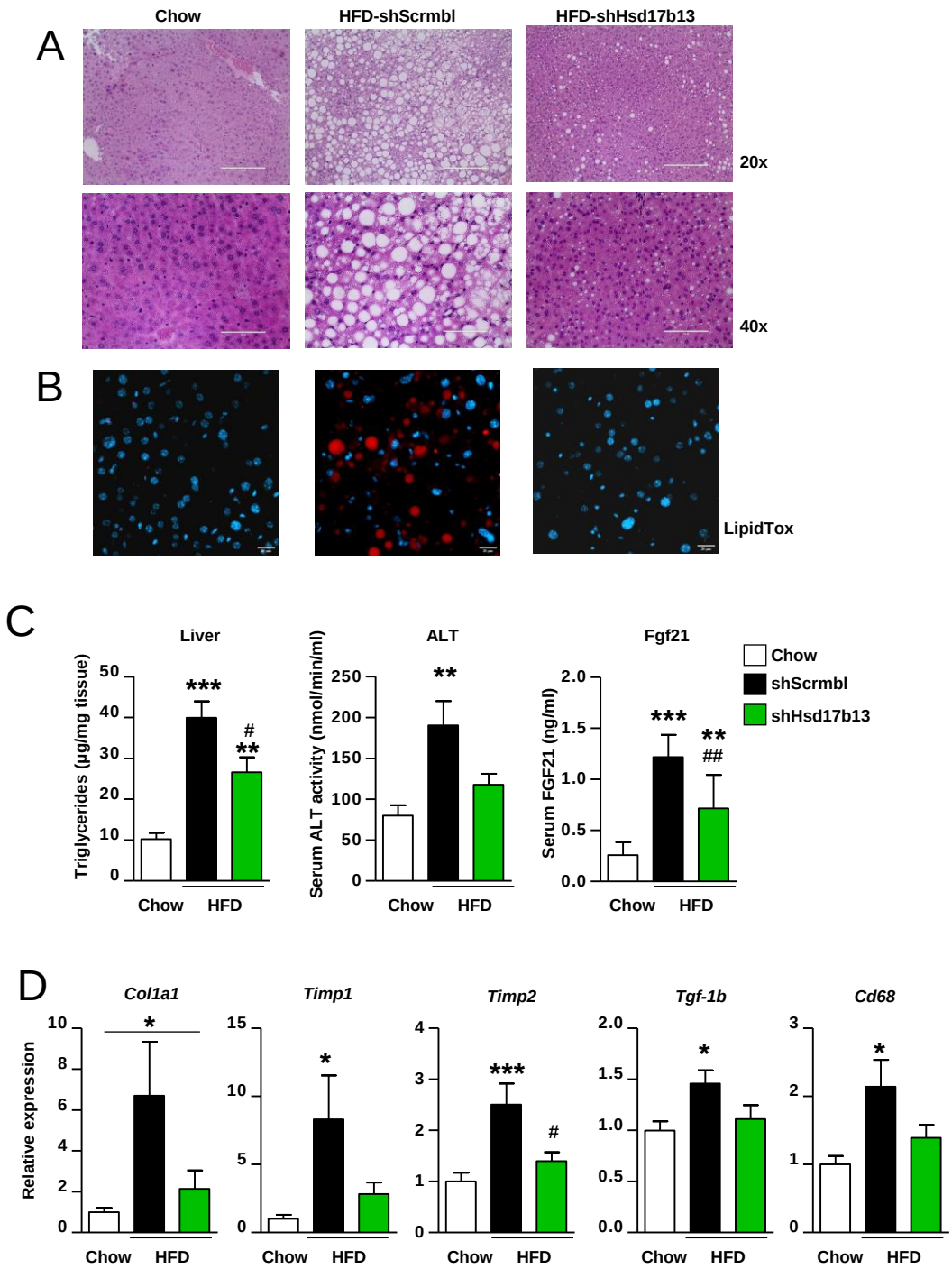
A
Chow
HFD-shScrmbl
HFD-shHsd17b13
20x
40x
B
LipidTox
C
Liver
Triglycerides (µg/mg tissue)
ALT
Serum ALT activity (nmol/min/ml)
Fgf21
Serum FGF21 (ng/ml)
Chow
shScrmbl
shHsd17b13
Chow
HFD
D
Col1a1
Timp1
Timp2
Tgf-1b
Cd68
Relative expression

FIGURE 5

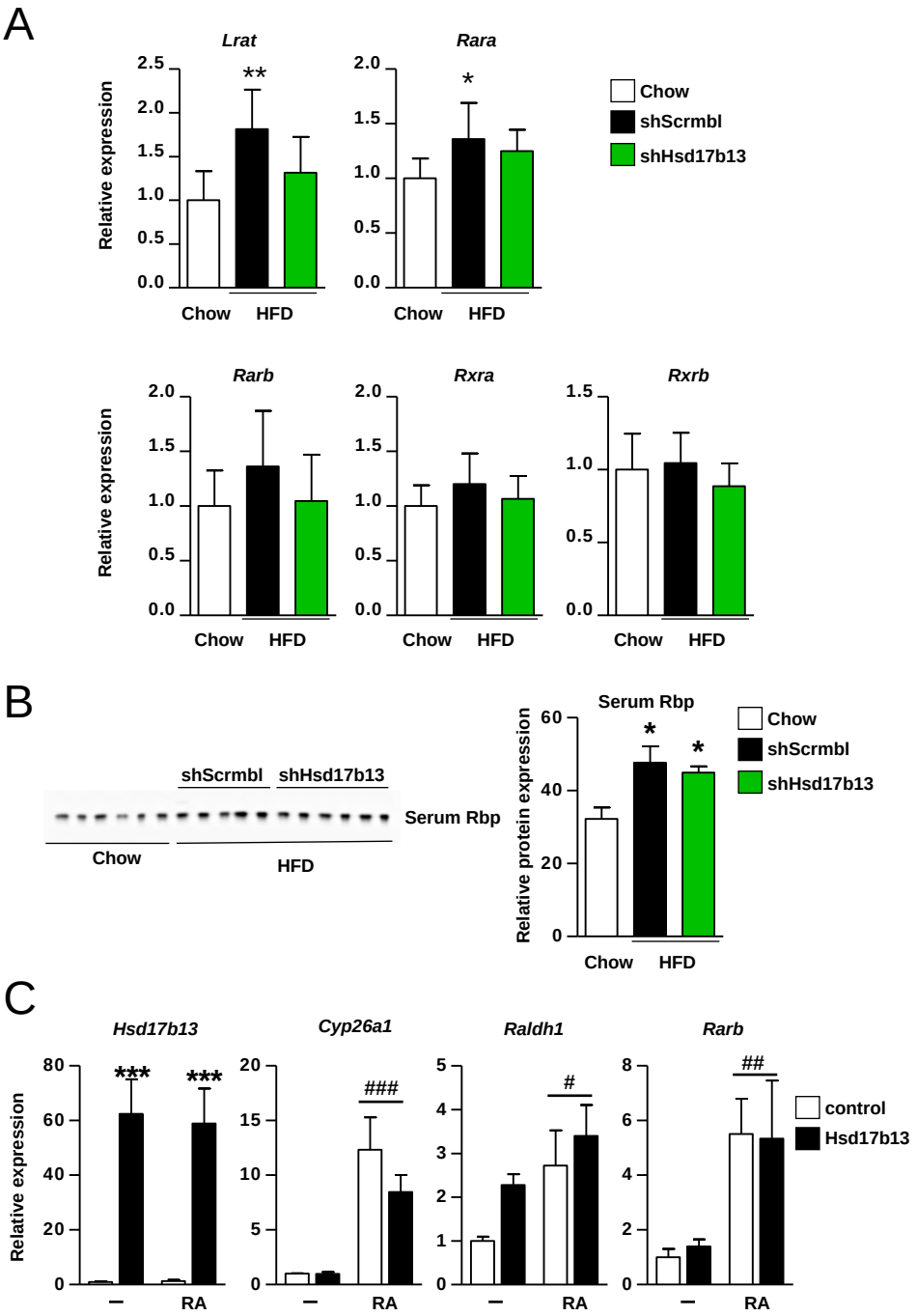
A
Lrat
Rara
Rarb
Rxra
Rxrb
Relative expression
Chow
HFD
shScrmbl
shHsd17b13
B
Serum Rbp
Relative protein expression
C
Hsd17b13
Cyp26a1
Raldh1
control
RA

FIGURE 6

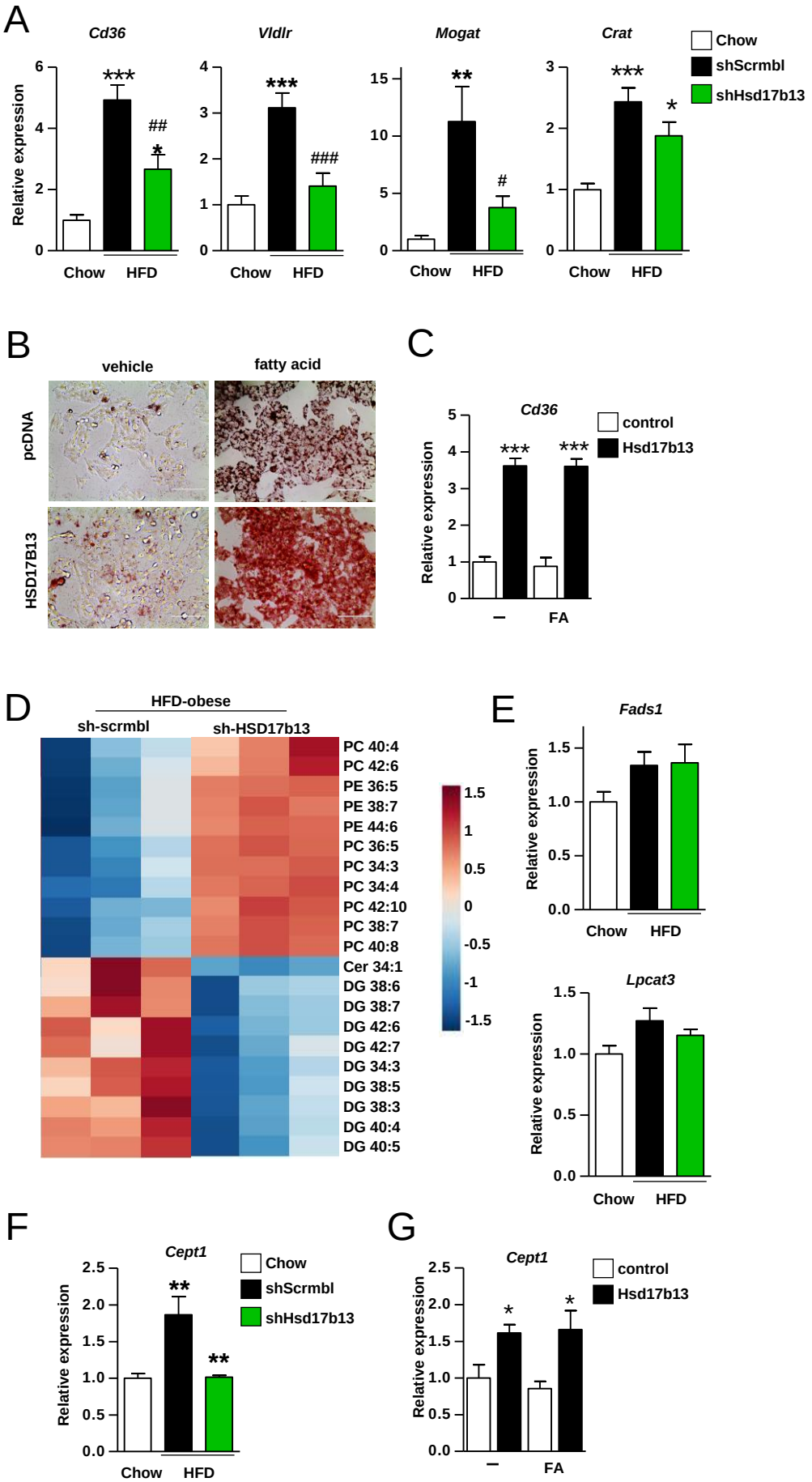
A
Cd36
Vldlr
Mogat
Crat
Chow
shScrmbl
shHsd17b13
Relative expression
Chow
HFD
B
vehicle
fatty acid
pcDNA
HSD17B13
C
Cd36
control
Hsd17b13
Relative expression
–
FA
D
HFD-obese
sh-scrmbl
sh-HSD17b13
PC 40:4
PC 42:6
PE 36:5
PE 38:7
PE 44:6
PC 36:5
PC 34:3
PC 34:4
PC 42:10
PC 38:7
PC 40:8
Cer 34:1
DG 38:6
DG 38:7
DG 42:6
DG 42:7
DG 34:3
DG 38:5
DG 38:3
DG 40:4
DG 40:5
E
Fads1
Lpcat3
F
Cept1
G